DGNSS Corrected Pseudorange and Time-Differenced Carrier Phase (TDCP) Measurements using Differentiable Factor Graph Optimization (DFGO)

Hoi-Fung Ng, *Department of Aeronautical and Aviation Engineering, The Hong Kong Polytechnic University*
Penghui Xu, *Department of Aeronautical and Aviation Engineering, The Hong Kong Polytechnic University*
Yihan Zhong, *Department of Aeronautical and Aviation Engineering, The Hong Kong Polytechnic University*
Guohao Zhang, *Department of Aeronautical and Aviation Engineering, The Hong Kong Polytechnic University*
Weisong Wen, *Department of Aeronautical and Aviation Engineering, The Hong Kong Polytechnic University*
Li-Ta Hsu, *Department of Aeronautical and Aviation Engineering, The Hong Kong Polytechnic University*

BIOGRAPHY

Hoi-Fung (Ivan) Ng is a PhD student in the Department of Aeronautical and Aviation Engineering, The Hong Kong Polytechnic University. He is a recipient of the Hong Kong PhD Fellowship. He received a B.Eng. in Air Transport Engineering and a M.Sc. in Mechanical Engineering from The Hong Kong Polytechnic University in 2018 and 2021 respectively. He is the awardee of the Student Paper Award in 2022 by the ION. His research interests include 3D mapping-aided GNSS positioning and navigation in urban canyons.

Penghui Xu received a B.S. degree from South China Agricultural University in 2015. In 2017, he obtained his MSc degree in mechanical engineering from The Hong Kong Polytechnic University. After that, he mainly works in machine learning algorithm development. Currently, he is pursuing a Ph.D. degree at The Hong Kong Polytechnic University. His research interests include machine learning, GNSS urban localization, and multi-sensor integration for positioning.

Yihan Zhong obtained his bachelor's degree in process equipment and control engineering from Guangxi University in 2020 and a Master's degree from The Hong Kong Polytechnic University (PolyU). He is currently a Ph.D. student at the Department of Aeronautical and Aviation Engineering (AAE) of PolyU. His research interests include factor graph optimization-based collaborative positioning and low-cost localization.

Guohao Zhang received his bachelor's degree in mechanical engineering and automation from University of Science and Technology Beijing, China, in 2015. He received his M.S. degree in Mechanical Engineering and his Ph.D. degree in Aeronautical and Aviation Engineering from the Hong Kong Polytechnic University. He is currently a Postdoctoral Research Fellow with the Department of Aeronautical and Aviation Engineering, the Hong Kong Polytechnic University. His research interests include GNSS urban positioning, collaborative positioning, and multi-sensor integrated navigation.

Weisong Wen received a Ph.D. degree in Mechanical Engineering from The Hong Kong Polytechnic University (PolyU), in Nov 2020. He was also a visiting Ph.D. student with the Faculty of Engineering, University of California, Berkeley (UC Berkeley) in 2018. In 2020, he won the Best Presentation Award from the Institute of Navigation (ION), and the First Prize in Hong Kong Section in Qianhai-Guangdong-Macao Youth Innovation and Entrepreneurship Competition, 2019. Before joining PolyU as a Research Assistant Professor in April 2021, he was a senior research fellow at PolyU. His research interests include GNSS positioning, SLAM, and collaborative positioning in challenging environments autonomous driving vehicles, and unmanned aerial vehicles.

Li-Ta Hsu is an associate professor at Department of Aeronautical and Aviation Engineering of Hong Kong Polytechnic University. He is Limin Endowed Young Scholar in Aerospace Navigation He received the B.S. and Ph.D. degrees in Aeronautics and Astronautics from National Cheng Kung University, Taiwan, in 2007 and 2013, respectively. He was a Visiting Researcher with the Faculty of Engineering, University College London and Tokyo University of Marine Science and Technology, in 2012 and 2013, respectively. In 2013, he won a Student Paper Award and two Best Presentation Awards from the Institute of Navigation (ION). He was selected as a Japan Society for the Promotion of Sciences Postdoctoral Fellow with the Institute of Industrial Science, The University of Tokyo and worked from 2014 to 2016. He is an Associate Fellow in the Royal Institute of Navigation. Dr. Hsu currently is members of ION and IEEE and serves as a member of the editorial board and reviewer in professional journals related to GNSS.

https://doi.org/10.33012/2024.19908

ABSTRACT

Google Smartphone Decimeter Challenge (SDC) provides a dataset for the communities to verify their leading-edge algorithm for precise smartphone GNSS positioning under the same baseline. This year's dataset provides more variety on the vendors of smartphones' GNSS chips, where the new data from affordable smartphones is believed to be noisier, increasing the position uncertainty. This study integrates the pseudorange, time-differenced carrier phase (TDCP) measurements, and estimated velocity using factor graph optimization (FGO) to provide an optimal and robust position estimation. In the optimization process, properly excluding and weighting the measurement is the key for only using healthy measurements for state estimation. This study also uses the differentiable FGO (DFGO) to determine the covariance for the GNSS positioning adaptively. The positioning results show that the network can provide a more robust and reliable performance than the traditional model-based approach.

I. INTRODUCTION

Android raw GNSS measurements have been provided since Android Release N (Nougat) and have powered over 2 billion devices since 2017 (Diggelen, 2017). Erroneous positioning performance can be studied and improved fundamentally with raw measurements, improving the reliability of smartphone positioning. Google Smartphone Decimeter Challenge (SDC) is the third year for GNSS community to test their leading-edge algorithm for precise smartphone GNSS positioning. In SDC 2022 (Fu et al., 2022), Dr Suzuki, champion of two years in a row, proposed a two-step approach to separate the velocity and position optimization process (Suzuki, 2022). Position and velocity are estimated via two separate factor graph optimization (FGO). The velocity outliers are excluded and interpolated, further adopted as a loose constraint for the proposed time-differenced carrier phase (TDCP) factor. The proposed framework achieves a horizontal positioning accuracy of 1.229 m.

The outstanding performance of the positioning framework proposed by Dr Suzuki in 2022 and 2023 inspires this study to follow a similar approach to tightly coupling pseudorange measurements, TDCP measurements, and estimated velocities. following the similar factor design in (Suzuki, 2022) and (Suzuki, 2023) is extended as the basis in this year's competition, we enhance the performance of the estimation by better estimating the covariance of the pseudorange and TDCP factors through the differentiable FGO (DFGO) (Xu et al., 2023). GNSS corrections are first generated by observations from continuously operating reference stations (CORS) as observation space representation (OSR), which is the lump sum of errors on satellite-related biases and atmospheric errors. DFGO then optimizes the position solution and weighting of each factor in a closed-loop manner. Position and velocity solutions are estimated by DFGO with input raw measurements and generated corrections. The outliers of the estimated velocity are excluded and interpolated for the training. Estimated solutions are then used to train the optimal covariance matrix of cost functions. Proposed end-to-end training for DFGO can adaptively determine the covariance for the GNSS positioning, outperforming the commonly used weighting from the measured uncertainty, showing its high potential positioning estimation.

This year's dataset added more GNSS chip vendors and smartphone models. It can be expected that the GNSS measurements are more noisy with outliers that affect the optimality of the optimization processes, especially for affordable smartphones. Therefore, it is worth studying the relationship of parameters across different devices. The training process and parameters adaptation are separated based on device-dependent strategies. Positioning performance is evaluated based on different devices and scenarios across weight schemes to show the relationship between them, where device-reported GNSS measurements' uncertainty might diverge based on their own confidence level.

The proposed approach uses datasets provided by SDC 2023 for evaluation and will be submitted to the competition on Kaggle. The positioning results show that the network can provide a more robust and reliable performance than the traditional model-based approach.

The contributions of this study include:

1. Integrates pseudorange, time-differenced carrier phase (TDCP) measurements, and estimated velocity using factor graph optimization (FGO).
2. Applies differentiable FGO (DFGO) to learn about the weighting for the optimization process.
3. Proposes outlier detection and exclusion schemes.

II. POSITIONING FRAMEWORK OUTLINE

This study uses a similar approach in (Suzuki, 2023) proposed. The flowchart of the proposed framework is shown in Figure 1.

The first step is to calculate GNSS measurement correction in OSR from the National Oceanic and Atmospheric Administration (NOAA) Continuously Operating Reference Stations (CORS) Network (NCN) (Galetzka et al., 2023). The estimated OSR correction applies to correct the pseudorange measurement. The corrected pseudorange measurements are used to estimate

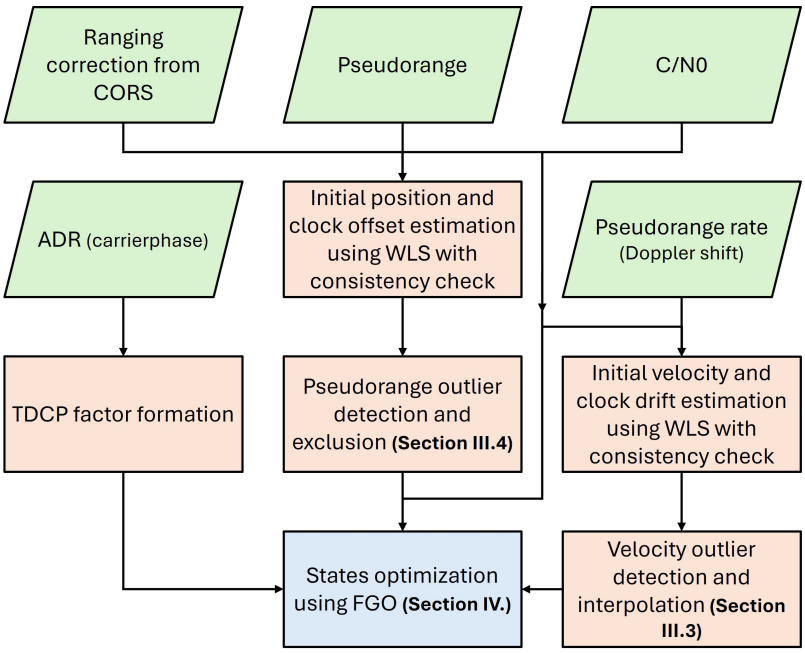

Figure 1: System chart of the positioning framework used in this study.

the position, $\mathbf{r}_{k,SPP}$, and clock offset, $\delta t_{k,SPP}$, of the receiver using least squares (LS) as a single-point positioning (SPP) approach. The state at epoch k, $\mathbf{x}_{k,SPP}$, of position and clock offset can be expressed as,

$$\mathbf{x}_{k,SPP} = \begin{bmatrix} \mathbf{r}_{k,SPP} \\ \delta \mathbf{t}_{k,SPP} \end{bmatrix}$$

$$\text{where} \quad \mathbf{r}_{k,SPP} = \begin{bmatrix} r_{k,x} & r_{k,y} & r_{k,z} \end{bmatrix}^\top \quad \text{and}$$

$$\delta \mathbf{t}_{k,SPP} = \begin{bmatrix} \delta t_k & \delta t_{k,\Delta GLOL1} & \delta t_{k,\Delta GALL1} & \delta t_{k,\Delta BDSL1} & \delta t_{k,\Delta GPSL5} & \delta t_{k,\Delta GLOL5} & \delta t_{k,\Delta GALL5} & \delta t_{k,\Delta BDSL5} \end{bmatrix}^\top \tag{1}$$

where $\delta t_{k,\Delta *}$ represents the relative clock offset of the $*$ constellation and signal to GPS L1. For example, "GLOL1" means the GLONASS L1 signal.

Meanwhile, the pseudorange rate, known as the Doppler shift, measures the smartphone's velocity, $\mathbf{v}_{k,SPP}$, and clock drift, $\dot{\delta \mathbf{t}}_{k,SPP}$.

$$\mathbf{x}_{k,\dot{\rho}} = \begin{bmatrix} \mathbf{v}_{k,\dot{\rho}} \\ \dot{\delta \mathbf{t}}_{k,\dot{\rho}} \end{bmatrix}$$

$$\text{where} \quad \mathbf{v}_{k,\dot{\rho}} = \begin{bmatrix} v_{k,x} & v_{k,y} & v_{k,z} \end{bmatrix}^\top \quad \text{and} \tag{2}$$

$$\dot{\delta \mathbf{t}}_{k,\dot{\rho}} = \begin{bmatrix} \dot{\delta t}_k & \dot{\delta t}_{k,\Delta GLOL1} & \dot{\delta t}_{k,\Delta GALL1} & \dot{\delta t}_{k,\Delta BDSL1} & \dot{\delta t}_{k,\Delta GPSL5} & \dot{\delta t}_{k,\Delta GLOL5} & \dot{\delta t}_{k,\Delta GALL5} & \dot{\delta t}_{k,\Delta BDSL5} \end{bmatrix}^\top$$

After that, the outlier of the estimated velocity is identified, and the outlier labelled velocity is interpolated; the detail is shown in section III.3. Another exclusion scheme is then applied to exclude pseudorange measurement using the estimated receiver clock offset and drift. The details of the outlier detection are introduced in section III.4.

Finally, the valid pseudorange, TDCP, and estimated velocity are inputted to the FGO to optimize the position estimates. The structure and involved cost functions are explained in section IV.

III. OUTLIER DETECTION AND EXCLUSION

1. GNSS Measurements

GNSS measurement outliers are identified and excluded from position estimation based on several conditions,

1. Any of the fields "TimeNanos", "ArrivalTimeNanosSinceGpsEpoch", "utcTimeMillis", and "FullBiasNanos" are invalid or equal to zero.
2. The field "ReceivedSvTimeUncertaintyNanos" is larger than 500 ns.
3. The field "ConstellationType" is equal to "CONSTELLATION_UNKNOWN" (0).
4. The field "MultipathIndicator" is set greater than 0.
5. The field "State" is not set for "STATE_CODE_LOCK" (1).
6. C/N_0 is less than 20 dB-Hz.
7. Satellite's position or velocity is empty or invalid.

In addition, pseudorange measurement is excluded from position estimation if the fields "RawPseudorangeMeters" or "RawPseudorangeUncertaintyMeters" are invalid or equal to zero. The pseudorange is also excluded if the device outputted uncertainty is greater than 150 m.

Similarly, pseudorange rate measurement is excluded from velocity estimation if the fields "PseudorangeRateMetersPerSecond" or "PseudorangeRateUncertaintyMetersPerSecond" are invalid or equal to zero.

ADR measurement is excluded from forming the TDCP factor in FGO if the pseudorange or pseudorange rate measurements are excluded. Besides, it is excluded if the fields "AccumulatedDeltaRangeMeters" or "AccumulatedDeltaRangeUncertaintyMeters" are invalid or equal to zero. Furthermore, the ADR measurement is excluded if the device outputted uncertainty is larger than 0.1 m. The ADR is invalid if the "AccumulatedDeltaRangeState" fulfils any of the following:

1. The ADR state is unknown.
2. The state is not set to "ADR_STATE_VALID" or "ADR_STATE_HALF_CYCLE_RESOLVED".
3. The state is set to "ADR_STATE_RESET".

The TDCP factor assumes that the ADR measurements of two consecutive epochs are free from cycle slip. Cycle slip detection is based on pseudorange rate and geometry-free combination in this study. The first cycle slip detection scheme is based on the differences between ADR measurements in TDCP and the pseudorange rate measurements. If the difference is larger than a certain threshold, the cycle slip flag is labelled. The detection can be expressed as,

$$\left| \left(\phi^i_{k+1} - \phi^i_k\right) - \frac{\Delta t}{2}\left(\dot{\rho}^i_k + \dot{\rho}^i_{k+1}\right) \right| < D_{\dot{\rho}} \tag{3}$$

where ϕ^i_k and ϕ^i_{k+1} are the ADR measurements in meter at epochs k and $k+1$, respectively. $\dot{\rho}^i_{k+1}$ and $\dot{\rho}^i_k$ are the pseudorange rate measurements in meter per second at epoch k and $k+1$, respectively. Δt is the time differences between epochs k and $k+1$. $D_{\dot{\rho}}$ is the determined threshold for cycle slip detection.

Another cycle slip detection scheme is geometric-free (GF) linear combination (LC). This only applies to the satellite that received both L1 and L5 frequencies of ADR measurement. Meanwhile, the ADR measurement of the corresponding satellite has to be also presented at the CORS station for detection. The detection can be expressed as,

$$\left| \left(\phi^i_{k+1,L1} - \phi^i_{k+1,L5}\right) - \left(\phi^i_{k,L1} - \phi^i_{k,L5}\right) \right| < D_{\phi,L1,L5} \tag{4}$$

where $\phi^i_{k+1,L1}$ and $\phi^i_{k+1,L5}$ are L1 and L5 band ADR measurements at epoch $k+1$, respectively. Similarly, $\phi^i_{k,L1}$ and $\phi^i_{k,L5}$ are L1 and L5 band ADR measurements at epoch k, respectively.

2. Consistency Check for Position and Velocity Estimation

A consistency check is also applied during the position estimation. Pseudorange measurement with the largest residual is excluded after each position estimation iteration. The measurement exclusion process terminates until one of the conditions is reached:

1. The largest pseudorange residual is smaller than a determined threshold, c_ρ.
2. The horizontal dilution of precision (HDOP) exceeds 1.0.
3. The degree of freedom of the problem is not fulfilled, such as the number of remaining measurements smaller than that of the unknown.

Similar to the position estimation, consistency check is applied to the velocity estimation. Termination conditions are as follows:

1. The largest ADR residual is smaller than a determined threshold, $c_{\dot{\rho}}$.
2. The horizontal dilution of precision (HDOP) exceeds 1.0.
3. The degree of freedom of the problem is not fulfilled, such as the number of remaining measurements smaller than that of the unknown.

3. SPP Estimated Velocity

If the SPP estimated velocity is detected to be an outlier, the velocity and clock drift are interpolated with the previous and next epochs'. Velocity outlier detection is based on three main conditions, where are:

1. The magnitude of the vertical component exceeded 15 m/s.
2. Total magnitude of all three axes exceeded 40 m/s.

4. Estimated Receiver Clock Offset Consistency

In SPP, the errors of pseudorange measurement are usually distributed to the estimated height and receiver clock offset. Estimated inter-constellation clock offset terms consist of the offset between the corresponding constellation and GPS L1-band in space segment and receiver internal delays. The inter-constellation clock offset should be relatively stable across periods, and this nature can be used to detect pseudorange outliers when a sudden jump occurs in the estimate. The first step is to calculate the average and standard deviation of the inter-constellation clock offset of a given constellation, s, notated as, $\mu_{\delta t,\Delta s}$ and $\sigma_{\delta t,\Delta s}$, respectively. GNSS measurement in constellation s indicates an outlier if the absolute difference between the value of "IsrbMeters", ε_{isrb}, and $\mu_{\delta t,\Delta s}$ is larger than the double of $\sigma_{\delta t,\Delta s}$, says,

$$|\varepsilon_{isrb} - \mu_{\delta t,\Delta s}| > 2 \times \sigma_{\delta t,\Delta s} \tag{5}$$

IV. FACTOR GRAPH OPTIMIZATION (FGO)

The position estimation step evaluates the state $\mathbf{x}_k$ that consists of position, r, and receiver clock offset, which can be expressed as,

$$\begin{gathered} \mathbf{x}_{k,FGO} = \begin{bmatrix} \mathbf{r}_k \\ \delta\mathbf{t}_k \end{bmatrix} \\ \text{where} \quad \mathbf{r}_k = [r_{k,x} \quad r_{k,y} \quad r_{k,z}]^\top \quad \text{and} \\ \delta\mathbf{t}_k = [\delta t_k \quad \delta t_{k,\Delta GLOL1} \quad \delta t_{k,\Delta GALL1} \quad \delta t_{k,\Delta BDSL1} \quad \delta t_{k,\Delta GPSL5} \quad \delta t_{k,\Delta GLOL5} \quad \delta t_{k,\Delta GALL5} \quad \delta t_{k,\Delta BDSL5}]^\top \end{gathered} \tag{6}$$

noted that the states are initialized by the SPP estimates, $\mathbf{x}_{k,SPP}$. FGO consists of the error factors on pseudorange, TDCP, and velocity with clock drift. The structure is shown in Figure 2.

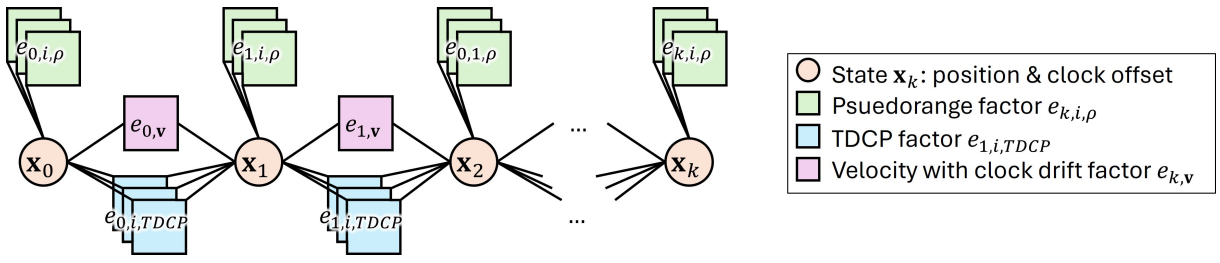

Figure 2: FGO structure for the positioning framework.

1. Pseudorange Factor

Pseudorange factor minimizes the differences between measured and modelled pseudorange, which can be expressed as,

$$\|e_{k,i,\rho}\|^2_{\sigma^{-1}_{k,i,\rho}} = \left\|\tilde{\rho}^i_k - \hat{\rho}^i(\mathbf{x}_k)\right\|^2_{\sigma^{-1}_{k,i,\rho}} \tag{7}$$

where $\sigma^{-1}_{k,i,\rho}$ is the error standard deviation of the corresponding pseudorange measurement. $\tilde{\rho}^i_k$ and $\hat{\rho}^i(\mathbf{x}_k)$ are measured and modelled pseudorange, respectively. The modelled pseudorange is expressed as,

$$\hat{\rho}^i(\mathbf{x}_k) = \left\|\mathbf{r}_k - \mathbf{r}^i_k\right\| + \delta t_k + \varepsilon^i_{k,OSR} \tag{8}$$

where $\|\mathbf{r}_k - \mathbf{r}^i\|$ represents the true range with Sagnac effect (Groves, 2013), calculated using the given satellite ECEF position, $\mathbf{r}^i$, and estimated ECEF position, $\mathbf{r}_k$. ε^i_{osr} is the ranging correction in OSR from CORS station, which is a lump sum of terms $-\delta t^i + I^i_k + T^i_k + \varepsilon^i_k$, and δt^i, I^i_k, and T^i_k are satellite clock delay, ionospheric delay, and tropospheric delay, respectively, provided in raw data file.ε^i_k denotes the non-modelled delays as a lump sum.

2. TDCP Factor

TDCP factor minimizes the error between ADR measurements and state changes in two consecutive epochs. It assumes no cycle slip in two consecutive ADR measurements, and the centimeter-level resolution can provide precise displacement between epochs. The error function is expressed as,

$$\|e_{k,i,TDCP}\|^2_{\sigma^{-1}_{k,i,TDCP}} = \left\|\left(\tilde{\phi}^i_{k+1} - \tilde{\phi}^i_k\right) - \left(\left\|\mathbf{r}_{k+1} - \mathbf{r}^i_{k+1}\right\| - \left\|\mathbf{r}_k - \mathbf{r}^i_k\right\| + \delta t_{k+1} - \delta t_k\right)\right\|^2_{\sigma^{-1}_{k,i,TDCP}} \tag{9}$$

where $\tilde{\phi}^i_k$ and $\tilde{\phi}^i_{k+1}$ are ADR measurements at epochs k and $k+1$, respectively. $\sigma^{-1}_{k,i,TDCP}$ is the average of the error standard deviation of the corresponding ADR measurements.

3. Velocity with Clock Drift Factor

The Velocity with clock drift factor links the positions of two successive epochs and minimizes the differences between the optimized position displacement and the estimated velocity from Doppler measurements. This factor can be expressed as,

$$\|e_{k,\mathbf{v}}\|^2_{\mathbf{\Sigma}^{-1}_{k,\mathbf{v}}} = \|(\mathbf{x}_{k+1,FGO} - \mathbf{x}_{k,FGO}) - \Delta t \times \mathbf{x}_{k,\dot{\rho}}\|^2_{\mathbf{\Sigma}^{-1}_{k,\mathbf{v}}} \tag{10}$$

where $\mathbf{\Sigma}_{k,\mathbf{v}}$ is the covariance matrix of the velocity estimated using WLS.

Finally, the FGO is formulated as,

$$\mathbf{\chi}^* = \arg\min_{\mathbf{\chi}} \sum_k \left\{ \sum_i \|e_{k,i,\rho}\|^2_{\sigma^{-1}_{k,i,\rho}} + \sum_i \|e_{k,i,TDCP}\|^2_{\sigma^{-1}_{k,i,TDCP}} + \|e_{k,\mathbf{v}}\|^2_{\mathbf{\Sigma}^{-1}_{k,\mathbf{v}}} \right\} \tag{11}$$

V. PERFORMANCE EVALUATION USING PROVIDED TRAINING DATASET

The positioning accuracy of different algorithms is evaluated using the provided training data. The information on each algorithm is summarised in Table 1.

Table 1: Information of evaluated algorithms.

Algorithm	Positioning basis	Measurement uncertainty	Consistency check	Ranging correction from CORS
1. Device output (baseline)	GNSS chip vendor	Unknow	Unknow	Unknow
2. SPP using device weighting	SPP	Device output	Yes	No
3. SPP using Sigma-ε weighting	SPP	Sigma-ε	Yes	No
4. SPP using DFGO weighting	SPP	DFGO	Yes	No
5. SPP using Sigma-ε weighting with OSR	SPP	Sigma-ε	Yes	Yes
6. FGO using device weighting	FGO	Device output	Yes	No
7. FGO using Sigma-ε weighting	FGO	Sigma-ε	Yes	No
8. FGO using DFGO weighting	FGO	DFGO	Yes	No
9. FGO using Sigma-ε weighting with OSR	FGO	Sigma-ε	Yes	Yes

Three measurement uncertainty schemes for GNSS measurement are used in this study, including:

1. Device output: device outputted measurements' uncertainties provided in CSV file.
2. Sigma-ε: C/N_0 based weighting scheme (Hartinger and Brunner, 1999). Parameter fitting is constellation- and signal type-dependent.
3. DFGO: An end-to-end training using differentiable FGO (Xu et al., 2023).

Positioning statistics are categorized based on the GNSS chip vendor and are summarized in Table 2. Each indicator refers to the average value across all training datasets. The score of each dataset is taking averages of the 50th and 95th percentile.

Table 2: Information of evaluated algorithms.

Algorithm	Indicator (m)	Qualcomm	Broadcom	Samsung LSI (Exynos)	MediaTek
1. Device output (baseline)	50-th percentile	2.62	2.41	402.03	2.48
	95-th percentile	5.70	5.66	24553.94	6.63
	Score	4.16	4.04	12477.98	4.55
2. SPP using device weighting	50-th percentile	2.44	2.50	2.89	2.54
	95-th percentile	5.38	5.98	8.05	7.03
	Score	3.91	4.24	5.47	4.79
3. SPP using Sigma-ε weighting	50-th percentile	2.29	2.37	2.88	2.49
	95-th percentile	5.17	5.16	7.74	6.34
	Score	3.73	3.82	5.31	4.41
4. SPP using DFGO weighting	50-th percentile	3.07	2.96	3.04	2.55
	95-th percentile	7.97	8.37	8.40	7.66
	Score	5.52	5.66	5.72	5.10
5. SPP using Sigma-ε weighting with OSR	50-th percentile	2.24	2.25	2.81	2.76
	95-th percentile	5.41	5.61	7.59	7.59
	Score	3.82	3.93	5.20	5.19
6. FGO using device weighting	50-th percentile	2.15	2.21	2.47	2.00
	95-th percentile	4.72	4.75	6.50	4.84
	Score	3.43	3.48	4.48	3.42
7. FGO using Sigma-ε weighting	50-th percentile	1.98	2.14	2.52	2.56
	95-th percentile	4.06	4.29	6.81	6.48
	Score	3.02	3.21	4.66	4.52
8. FGO using DFGO weighting	50-th percentile	2.00	2.19	2.44	2.04
	95-th percentile	4.85	5.12	6.37	5.12
	Score	3.42	3.65	4.40	3.58
9. FGO using Sigma-ε weighting with OSR	50-th percentile	1.99	2.33	2.70	2.80
	95-th percentile	4.03	4.72	7.00	7.46
	Score	3.01	3.53	4.85	5.13

Several conclusions can be drawn from the results, which can be categorized on measurement selection and weighting, positioning basis, or device basis. Starting from measurement selection, a consistency check is important for outlier exclusion. Comparing algorithms 1 and 2, positioning accuracy improved after excluding measurement outliers from position estimation, especially for the Samsung LSI chip. Furthermore, correctly weighting the healthiness of measurements is important for precise positioning. Using the Sigma-ε weighting scheme can achieve the best positioning accuracy. However, positioning performance on MediaTek became worse when using the Sigma-ε weighting scheme. The reason could be limited samples for fitting the weights.

For the positioning basis, FGO outperforms SPP in positioning accuracy in general. FGO improved the score by at least 0.5 m compared to SPP under the identical corresponding weighting scheme. This shows that solving the state as batch optimization can achieve more precise positioning.

Compared to the positioning performance of different chip vendors, Qualcomm and Broadcom have better positioning performance than Samsung LSI and MediaTek. From standard deviation (STD) of the labelled pseudorange residuals shown in Figure 3, MediaTek has a smaller STD in general, but some of the C/N_0 does not lie on the curve, especially for Beidou (BDS) L1, making the fitting not perfect enough to predict the healthiness of the measurement.

Based on the current FGO positioning framework results, selecting healthy pseudorange measurements and weighing them is the key to determining a good absolute position. An example is shown in Figure 4. The vehicle remains static at the beginning

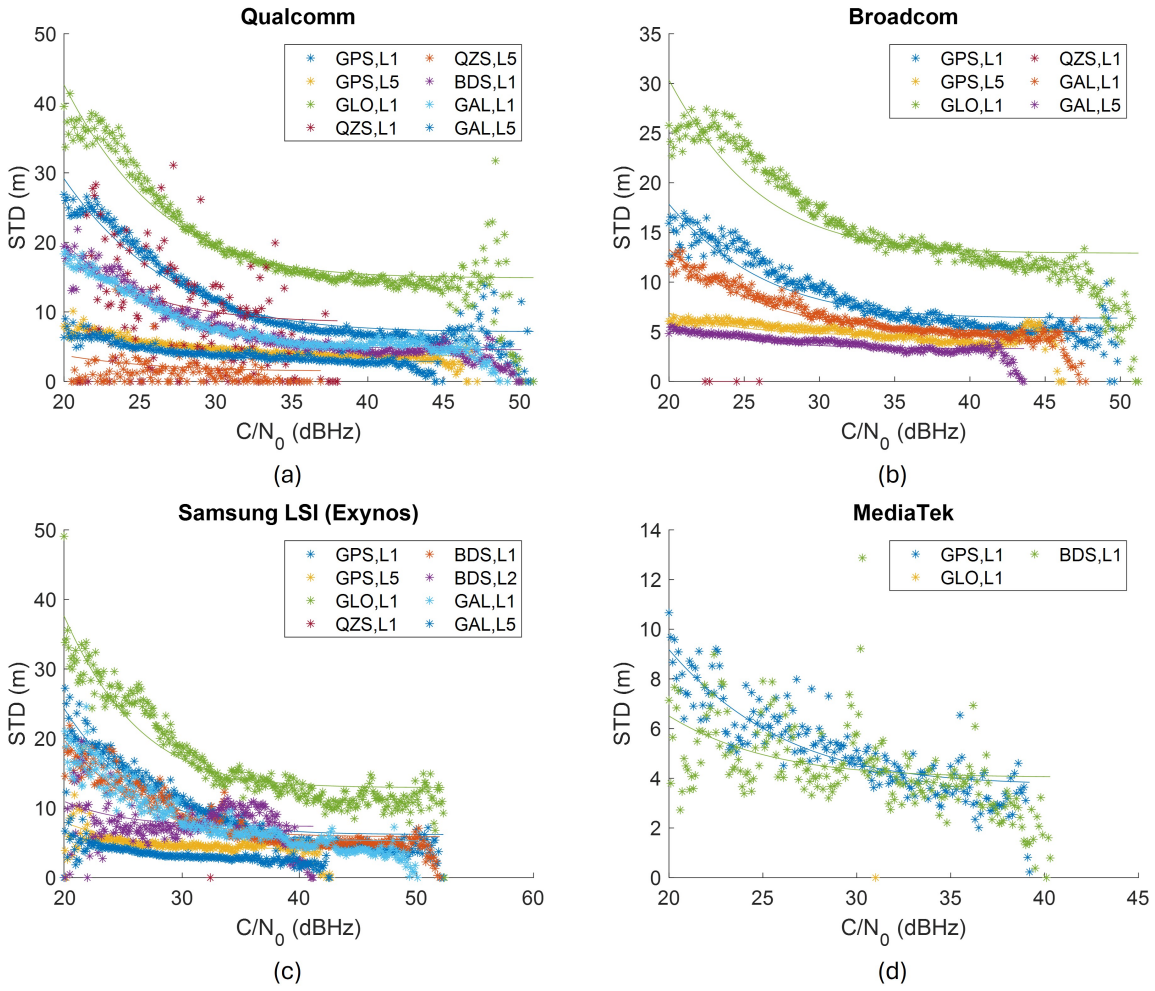

Figure 3: Standard deviation (STD) of the labelled pseudorange residuals for each GNSS chips vendor: (a) Qualcomm; (b) Broadcom; (c) Samsung LSI (Exynos); and (d) MediaTek. Solid lines represent the fitted curve for the Sigma-ε weighting scheme.

of the run, though the relative position or velocity estimates are with low error, the whole trajectory shifts at the beginning due to the positioning error at the starting point.

VI. CONCLUSIONS AND FUTURE WORK

This study proposed a smartphone positioning framework based on FGO with measurement selection and ranging correction from CORS. The framework development is based on a two-step approach proposed by Dr Suzuki 2023. The first step is estimating the initial states on position, velocity, clock offset, and clock drift using LS with consistency check. After that, the velocity outliers are excluded and interpolated. Besides, pseudorange outliers are excluded if the ISRB of the corresponding measurement is inconsistent with the estimated inter-constellation clock offset. Finally, valid pseudorange, TDCP measurements, and estimated velocities are added to FGO to estimate the positions and clock offsets. Train data is used to evaluate the performance of different positioning algorithms. The results show that FGO can provide better positioning performance. Furthermore, selecting and weighting healthy measurements are important for FGO, and outlier exclusion, and Sigma-ε can provide the best positioning performance.

Several possible improvements can be made based on the current positioning framework. The first change is increasing the connections of the ADR measurement from TDCP to the window carrier phase (WCP) (Bai et al., 2022). This can increase the robustness of the carrier phase measurement from the affection of the undetected cycle slip. The second improvement is to extend the ranging corrections from single station to multiple stations to increase the redundancy. Furthermore, the improvement of the current DGNSS is not significant, so further study on the implementation of the ranging correction is needed.

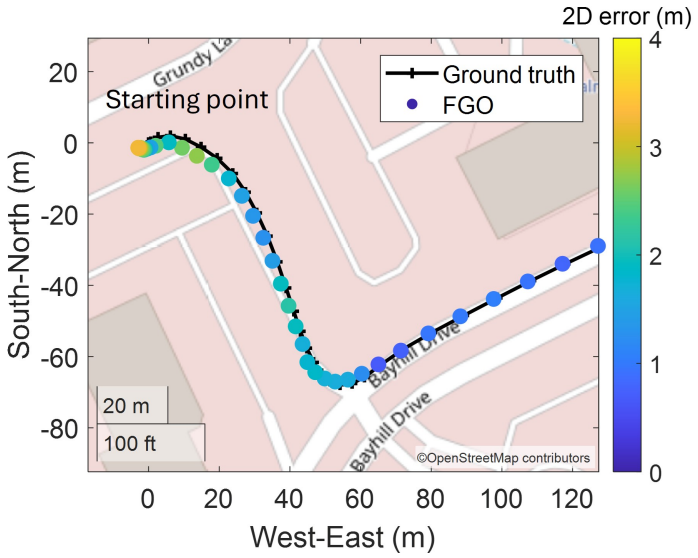

Figure 4: Example of the FGO result on dataset "2020-07-08-22-28-us-ca; pixel4xl".

REFERENCES

Bai, X., Wen, W., and Hsu, L.-T. (2022). Time-correlated window-carrier-phase-aided gnss positioning using factor graph optimization for urban positioning. *IEEE Transactions on Aerospace and Electronic Systems*, 58(4):3370 – 3384.

Diggelen, F. v. (2017). Google analysis tools for gnss raw measurements, g.co/gnsstools. In *Proceedings of the 30th International Technical Meeting of the Satellite Division of The Institute of Navigation (ION GNSS+ 2017)*, pages 345 – 356, Portland, Oregon.

Fu, M., Khider, M., and Diggelen, F. v. (2022). Summary and legacy of the smartphone decimeter challenge (sdc) 2022. In *Proceedings of the 36th International Technical Meeting of the Satellite Division of The Institute of Navigation (ION GNSS+ 2023)*, pages 2301 – 2320, Denver, Colorado.

Galetzka, J., Sellars, I., Freeman, W., Coloma, F., Haw, D., Sun, L., and Saleh, J. (2023). The noaa cors network (ncn): A brief history and current status.

Groves, P. D. (2013). *Principles of GNSS, inertial, and multisensor integrated navigation systems, Second Edition*. Artech House, 2nd edition.

Hartinger, H. and Brunner, F. (1999). Variances of gps phase observations: The sigma- model. *GPS Solutions*, 2:35 – 43.

Suzuki, T. (2022). 1st place winner of the smartphone decimeter challenge: Two-step optimization of velocity and position using smartphone's carrier phase observations. In *Proceedings of the 35th International Technical Meeting of the Satellite Division of The Institute of Navigation (ION GNSS+ 2022)*, pages 2276 – 2286, Denver, Colorado.

Suzuki, T. (2023). Precise position estimation using smartphone raw gnss data based on two-step optimization. *Sensors*, 23(3):1205.

Xu, P., Ng, H.-F., Zhong, Y., Zhang, G., Wen, W., Yang, B., and Hsu, L.-T. (2023). Differentiable factor graph optimization with intelligent covariance adaptation for accurate smartphone positioning. In *Proceedings of the 36th International Technical Meeting of the Satellite Division of The Institute of Navigation (ION GNSS+ 2023)*, pages 2765 – 2773, Denver, Colorado.